Research Square

Preprints are preliminary reports that have not undergone peer review.
They should not be considered conclusive, used to inform clinical practice,
or referenced by the media as validated information.

Spatiotemporal variation in soil CO2 flux in conserved and degraded sectors of a high-Andean bofedal in Puno, Peru

Mario Flores-Aroni

marioflores@unap.edu.pe

National University of Altiplano, Puno

Alcida Lourdes Chua Mamani

National University of Altiplano, Puno

José Henrique Cattanio

Federal University of Pará

Research Article

Keywords: Altiplano, bofedal degradation, grazing, high-Andean peatland, water table, soil respiration

Posted Date: November 25th, 2026

DOI: https://doi.org/10.21203/rs.3.rs-11775938/v1

License: This work is licensed under a Creative Commons Attribution 4.0 International License.
Read Full License

Additional Declarations: No competing interests reported.

Spatiotemporal variation in soil CO_2 flux in conserved and degraded sectors of a high-Andean bofedal in Puno, Peru

Mario Flores-Aroni[1,2*], Alcida Lourdes Chua Mamani[1], José Henrique Cattanio[2,3]

[1] Faculty of Agricultural Sciences, Professional School of Agricultural Engineering, National University of Altiplano, Puno, Peru

[2] Graduate Program in Environmental Sciences, Federal University of Pará, Belém, Brazil

[3] Biogeochemical Cycles Laboratory, Federal University of Pará, Belém, Brazil

ORCID: Mario Flores-Aroni, https://orcid.org/0000-0002-1206-0743; Alcida Lourdes Chua Mamani, https://orcid.org/0009-0004-4086-7554; José Henrique Cattanio, https://orcid.org/0000-0001-8335-9593

* Correspondence: marioflores@unap.edu.pe

Abstract

High-Andean bofedales (cushion-plant peatlands) store large amounts of organic carbon, but overgrazing and altered hydrology may turn them into sources of carbon dioxide (CO_2). We assessed the spatiotemporal variation of soil CO_2 flux (FCO_2) in conserved and degraded sectors of a bofedal in Jila Cajamarca (Puno, Peru; 4,480 m a.s.l.) and its relationship with soil and micrometeorological variables. The ecological condition of six sites (S1-S6) was evaluated following the guidelines of the Peruvian Ministry of the Environment, and FCO_2 was measured with a dynamic closed chamber and a portable infrared gas analyzer in 12 campaigns (August 2025 to March 2026; n = 432) and analyzed with repeated-measures linear mixed models. Conserved sites were classified as "Good" (S4-S6) and degraded sites as "Fair" (S2 and S3) and "Poor" (S1). FCO_2 was 23.6% higher in degraded (1.10 ± 0.05 g CO_2 m^{-2} h^{-1}) than in conserved sectors (0.89 ± 0.04 g CO_2 m^{-2} h^{-1}; $p = 0.027$) and varied among dates, with no condition × date interaction; the degraded mean was higher in all 12 campaigns. Soil properties did not differ between conditions, but degraded sectors had a deeper water table (26.5 vs. 7.4 cm) and thinner peat (91.1 vs. 138.5 cm). FCO_2 was positively associated with relative humidity and negatively with organic matter, whereas its weak association with soil temperature did not persist when soil temperature was included as a covariate. Bofedal degradation was associated with higher daytime soil CO_2 emissions, suggesting that conservation and hydrological restoration could help reduce them.

Keywords: Altiplano, bofedal degradation, grazing, high-Andean peatland, water table, soil respiration

Introduction

The increase in atmospheric concentrations of greenhouse gases (GHGs), particularly carbon dioxide (CO_2), is the primary driver of observed global warming (IPCC 2021). Soil respiration, which integrates root and microbial activity, constitutes one of the largest carbon fluxes between the terrestrial biosphere and the atmosphere, and its magnitude depends on temperature, moisture, substrate quality, and soil management (Raich and Schlesinger 1992; Davidson et al. 2000). In peatlands, however, water table position acts as the dominant control because it modulates oxygen availability and, consequently, the rate of organic matter decomposition (Evans et al. 2021). Under warmer conditions or altered water availability, soils may shift from carbon reservoirs to carbon sources (Davidson and Janssens 2006; Flores et al. 2025).

Peatlands occupy approximately 3% of the global land surface but store a disproportionately high share of soil organic carbon (Ramsar 2018). When drained, they become net GHG sources, making their conservation and rewetting a frequently underestimated climate mitigation strategy (Leifeld and Menichetti 2018). In the tropical Andes, mountain peatlands accumulate thick carbon deposits, with a mean of approximately 1,743 Mg C ha^{-1}, one to two orders of magnitude greater than the carbon stored in mineral soils of the same region, and their long-term accumulation depends primarily on elevation and temperature, rendering them especially vulnerable to warming (Hribljan et al. 2024). In the Peruvian Altiplano, these peatlands are known as bofedales: high-Andean wetlands dominated by cushion plants that sustain base flows and provide forage for camelid livestock (Maldonado 2014; MINAM 2019; Huaman et al. 2020). In the Puna of the central Andes, their persistence depends on continuous water inputs and is threatened by overgrazing, water diversion, and climate change (Oyague and Cooper 2020).

The functioning of bofedales depends on the persistence of a water table near the surface, which maintains anoxic conditions and slows organic matter (OM) decomposition (Cooper et al. 2019; Monge-Salazar et al. 2022). Water table position also determines whether CO_2 production (aerated soils) or methane production (saturated soils) predominates (Huang et al. 2021; Flores et al. 2026). Overgrazing, trampling, drainage ditch excavation, and hydroclimatic changes disrupt this balance (Anderson et al. 2021). In the Cordillera Blanca, drainage of mountain peatlands converted carbon sinks into CO_2 sources (Planas-Clarke et al. 2020), whereas in the Ecuadorian páramo, grazing alters CO_2 exchange and increases methane emissions (Sánchez et al. 2017). Globally, water table depth is the primary control on net GHG emissions from disturbed peatlands (Evans et al. 2021).

However, the response of soil respiration to degradation is not uniform, and available studies report contrasting results. In alpine wetlands of the Tibetan Plateau, degradation reduced soil respiration and its thermal sensitivity owing to the loss of plant biomass and organic carbon (Li et al. 2019), whereas in Peruvian Amazonian peatlands, degradation increased CO_2 emissions, with a maximum at intermediate soil moisture levels (Lent et al. 2019). In cold South American ecosystems, soil temperature explains much of the variation in CO_2 flux (Sá et al. 2019), but in saturated soils, water may limit oxygen diffusion and decouple respiration from the thermal regime (Davidson et al. 2000; Flores et al. 2025). This divergence of responses underscores the need to assess degradation effects in specific contexts where edaphic properties and hydrological regime may modulate both the sign and magnitude of change.

In the Puno region, studies on soil CO_2 flux in high-Andean wetlands are recent and have focused on seasonal and among-site variation (Checalla 2023; Mamani 2024; Nuñez 2024; Flores-Aroni et al. 2025). In the Inner Bay of Puno, flux varies between seasons and zones and correlates with air and soil temperature (Flores-Aroni et al. 2025). However, none of these studies compared sectors with differing conservation status; consequently, the extent to which degradation modifies the magnitude and temporal variability of soil CO_2 flux in Altiplano bofedales, and which edaphic properties mediate this effect, remain unknown. This temporal variability is particularly important because it determines the representativeness of point measurements and the uncertainty of carbon inventories, whose default emission factors for organic soils were derived mainly from lowland peatlands (IPCC 2014). We hypothesized that degradation, by reducing peat water saturation, increases soil CO_2 flux and its temporal variability.

The objective of this study was to evaluate the spatiotemporal variation of soil CO_2 flux in conserved and degraded sectors of a high-Andean bofedal in Puno, and to determine its relationship with edaphic properties and micrometeorological variables. To test this hypothesis, sectors were classified according to their vegetation conservation status and hydrological regime.

Materials and methods

Study area

The study was conducted in a bofedal (high-Andean peatland) in the community of Jila Cajamarca, Potoni District, Azángaro Province, Puno, Peru (14°26′38.09″ S, 70°10′15.29″ W; 4,480 m a.s.l.; Fig. 1). The diurnal temperature range is wide, with maximum temperatures of 18 °C and minima reaching -10 °C

in winter. Precipitation is concentrated between December and March, with a mean annual total of 600-750 mm (SENAMHI 2026). The bofedal covers approximately 40 ha and is used for grazing camelids and sheep. According to the Köppen-Geiger classification, the regional climate is high-mountain tundra (ET), with a well-defined dry season from May to November (Beck et al. 2018).

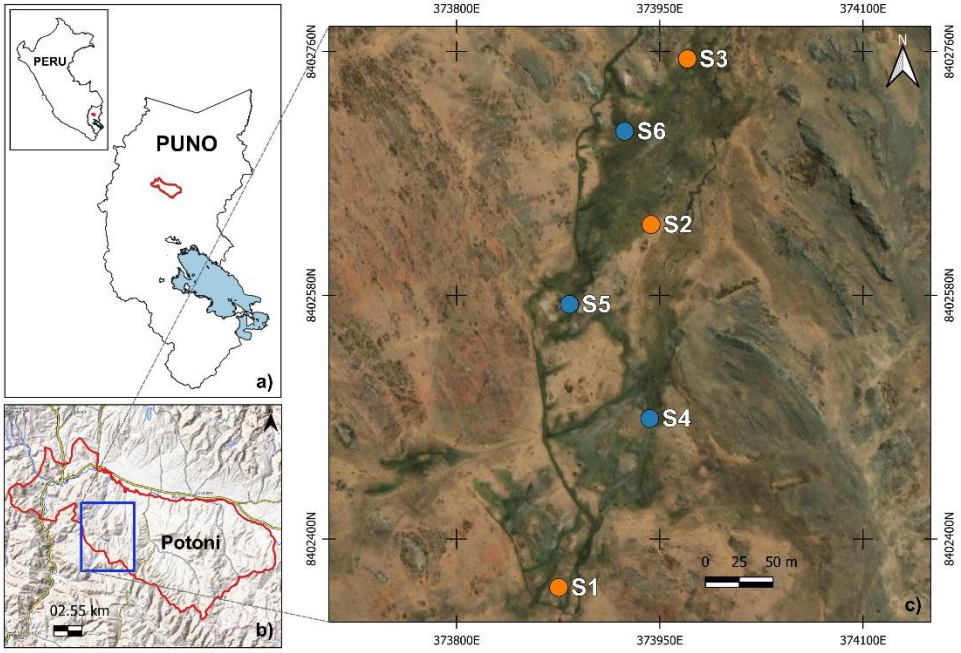

Fig. 1 Location of sampling sites in the bofedal of the Jila Cajamarca community, Potoni District, Azángaro, Puno, Peru. Degraded sites: S1, S2, S3; conserved sites: S4, S5, S6

Sampling site selection

Three sites were selected per conservation condition (degraded and conserved), with six collars per site, yielding 36 measurements per date and 432 over the 12 campaigns (Fig. 1; Online Resource 1, Table S1). The distance from each site to its nearest neighbor ranged from 68 to 139 m (mean ≈ 90 m); the maximum distance between sites was approximately 400 m, and collars within each site were spaced 5 m apart to capture spatial heterogeneity. Sites were located at comparable topographic positions (slope < 5%) to minimize the effect of relief on the hydrological regime.

Assessment of the current condition of high-Andean bofedales

Bofedal condition was assessed using the procedures of the *Guía de evaluación del estado del ecosistema de bofedal* [Guide for Assessing the Condition of the Bofedal Ecosystem] (MINAM 2019), which integrates the attributes and indicators listed in Table 1. Each indicator received a relative value, and the

sum of these values defined the total score and condition category for each site. Sites were classified as conserved or degraded according to the thresholds established in this guide; specifically, sites with a relative value > 60% (categories "Good," 60.1-80%, and "Very good," > 80%) were considered conserved, and sites with a value ≤ 60% (categories "Fair," 40.1-60%, and "Poor," 20.1-40%) were considered degraded. The assessment was performed once, at the beginning of the study, and condition was assumed to remain stable throughout the measurement period. The proportion of native species and species richness were recorded using the point-intercept method every 50 cm along a 50-m transect per site (100 points); live vegetation cover was estimated visually in 1 × 1 m quadrats located at 12.5, 25, and 37.5 m along the transect, and aboveground biomass was determined by clipping vegetation in 25 × 25 cm quadrats and oven-drying it at 105 °C to constant weight (MINAM 2019). In addition, the bofedal survey form from the same guide was completed for each site, recording litter cover and dominant, subdominant, and associated species according to their relative cover.

Table 1 Attributes and indicators used to assess the condition of the bofedal ecosystem

Attributes	**Indicators**
Water condition	Dry-season water table depth (cm); electrical conductivity (mS cm^{-1})
Soil condition	Peat depth (cm); organic matter (%); bulk density (g cm^{-3}); signs of erosion (qualitative)
Biotic condition	Native species (%); species richness (no. species per area); live vegetation cover (%); aboveground biomass (kg DM ha^{-1})
Landscape alterations	Presence of degradation factors (qualitative); hydrological connectivity of the bofedal (qualitative)

Note. Adapted from MINAM (2019).

Measurement of carbon dioxide flux

PVC collars were placed randomly within each site, inserted 3-4 cm into the soil two days before the first measurement to allow the soil to stabilize, and remained in place throughout the study. Collars were 10 cm in diameter and 10 cm in height, with 6-7 cm remaining above the soil surface.

Soil CO_2 flux was measured with a dynamic closed respiration chamber (SRC-1, PP Systems, USA) coupled to an infrared gas analyzer (EGM-4, PP Systems). This technique has previously been used with the same equipment in wetlands of Puno (Flores-Aroni et al. 2025). Before each campaign, analyzer calibration was verified with a reference gas, and the equipment performed an auto-zero before each measurement. Each measurement lasted two minutes, during which the increase in CO_2 concentration

inside the chamber was recorded. Twelve campaigns were conducted between 10 August 2025 and 17 March 2026, at approximately 20-day intervals, between 09:00 and 14:00 h, always in the same order from south to north (S1, S4, S5, S2, S6, S3), so that both conditions were interspersed throughout each campaign.

Calculation of soil carbon dioxide flux

Soil CO_2 flux was estimated from the linear change in CO_2 concentration inside the closed chamber over time, based on the ideal gas law (Metcalfe et al. 2007; Marthews et al. 2014). Linearity of the concentration-time curve was verified for each measurement, and records with $R^2 < 0.90$ or evident disturbances were discarded. No record met these criteria; therefore, all 432 measurements (36 collars × 12 dates) were analyzed. Uncorrected (Fs) and corrected (Fsc) CO_2 flux were calculated as:

$$Fs = \left(\frac{Cn-C1}{tn-t1}\right)\left(\frac{P}{Ta}\right)\left(\frac{Vd}{A}\right)\left(\frac{44.01 \times 0.36}{R}\right) \quad (1)$$

$$Fsc = Fs\left(\frac{Vd+Vc}{Vd}\right) \quad (2)$$

where Fs and Fsc are uncorrected and corrected CO_2 flux (g CO_2 m^{-2} h^{-1}); Cn - C1 is the difference in CO_2 concentration in the chamber (ppm); tn − t1 is the time difference (s); P is atmospheric pressure (hPa); Ta is air temperature inside the chamber (K); Vd is the internal volume of the SRC-1 chamber (m^3); A is the soil area covered by the chamber (m^2); R is the gas constant (8.314 J K^{-1} mol^{-1}); Vc is the collar volume above the soil (m^3); and 44.01 is the molecular mass of CO_2 (g mol^{-1}). The factor 0.36 results from 10^{-6} (ppm to mol mol^{-1}) × 10^2 (hPa to Pa) × 3,600 (s to h). For reference, 1 g CO_2 m^{-2} h^{-1} is equivalent to 6.31 µmol CO_2 m^{-2} s^{-1}. All fluxes reported in this study correspond to Fsc.

Soil sampling and analysis

At each flux measurement site, three soil samples were collected at 0-10 cm depth and analyzed at the INIA-Puno laboratory. Samples were collected on 10 August 2025 (at the start of the in situ monitoring period) and stored at 4 °C until processing. pH was determined by potentiometry in a 1:2.5 soil:water suspension; electrical conductivity (EC) by conductometry in the aqueous extract; and bulk density (BD) by the volumetric ring method, with samples dried at 105 °C to constant weight (Embrapa 2017). Organic carbon was determined by the Walkley and Black (1934) method, and OM was obtained using the factor 1.724 (Kalra and Maynard 1991). This factor assumes that OM contains 58% carbon and tends to underestimate OM; a factor close to 2 has been proposed for most soils (Pribyl 2010). Peat depth was

measured with a 10.2-cm (4-inch) diameter auger until the mineral substrate was reached. Water table depth was measured at each site in the hole opened with the auger: once the water level stabilized, the vertical distance between the soil surface and the water table was recorded with a tape measure fitted with a contact sensor.

Soil moisture and temperature

Two soil samples per site (0-10 cm) were collected on each date and dried at 105 °C to constant weight. Gravimetric soil moisture (SM, dry-weight basis) was calculated as SM = [(Mh − Ms)/Ms] × 100, where Mh and Ms are the wet and dry mass of the sample (g), respectively. A precision digital thermometer (TP300) was used to record soil temperature (ST) at each collar at 4 cm depth simultaneously with flux measurement.

Micrometeorological variables

Relative humidity (RH, %), atmospheric pressure (P, hPa), air temperature (Tair, °C), and wind speed (Ws, m s^{-1}) were recorded with a multifunctional digital anemometer (GM 8910), with two records per site on each measurement date. Measurements were made at 1.5 m above the soil surface and concurrently with flux measurements.

Statistical analysis

Soil CO_2 flux (FCO_2) was analyzed without transformation using a linear mixed-effects model for repeated measures (equivalent to a repeated-measures ANOVA), with date, condition, and their interaction as fixed effects. Site was the experimental unit (n = 3 per condition), and chambers were treated as subsamples rather than independent replicates (Hurlbert 1984). The model included a correlation structure for successive measurements on the same chamber and heterogeneous variances by condition, both selected using the Akaike information criterion (AIC), following the approach used in the Amazon estuary (Flores et al. 2026). Condition was evaluated with an F test with 1 and 4 degrees of freedom, and dates were compared with Tukey's test ($\alpha = 0.05$); the difference between conditions is expressed with its 95% confidence interval (95% CI). The same model was applied to ST, SM, and micrometeorological variables. Soil properties (n = 18 samples) were compared with a mixed model with site as a random effect, and water table depth and peat depth, measured once per site, with a one-way analysis of variance (F test with 1 and 4 degrees of freedom); the relationship between the two was evaluated with Pearson correlation (n = 6). The relationship of FCO_2 with each variable was evaluated

with repeated-measures correlation (r_{rm}; Bakdash and Marusich 2017), which measures association within each chamber, recording position, or site without conflating it with between-site differences. In addition, each variable was standardized and included separately as a covariate in the mixed model of FCO_2 (β: change in flux per standard deviation). For soil properties, the mean FCO_2 of the two chambers associated with each sample was used. Analyses were performed in R (R Core Team 2025), using the nlme, emmeans, and rmcorr packages.

Results

Current condition of the high-Andean bofedal

The assessment classified the three conserved sites as "Good" (S4 = 69.7; S5 = 76.5; S6 = 68.7) and the degraded sites as "Fair" (S2 = 41.7; S3 = 45.6) and "Poor" (S1 = 38.5). S1, the only site in "Poor" condition, had the deepest water table (36.2 cm), the thinnest peat (88.4 cm), category D erosion signs, and the lowest species richness (6), and also recorded the highest site-date mean FCO_2 of the study (1.76 g CO_2 m^{-2} h^{-1}, 26 February 2026). Conserved sites scored higher for dry-season water table depth, peat depth, native species, live vegetation cover, and absence of degradation factors (Table 2). Floristic composition also differed between conditions (Online Resource 1, Table S5). In sites in "Good" condition, *Festuca dolichophylla* dominated, with the cushion plants *Oxychloe andina* and *Distichia muscoides* as subdominants and *Carex* sp., *Eleocharis* sp., and *Calamagrostis* sp. as associated species; this was also the only condition in which litter was recorded (32.6%). In "Fair" sites, *Plantago tubulosa* dominated, followed by mosses, with *Oxalis* sp., *Carex* sp., and *Calamagrostis* sp. as associated species, whereas in S1 ("Poor"), *Phylloscirpus deserticola* and *Plantago tubulosa* dominated, with mosses and *Oxalis* sp. as subdominants. Mean aboveground biomass decreased from 1,526 kg DM ha^{-1} in "Good" sites to 1,096 kg DM ha^{-1} in "Fair" sites and 960 kg DM ha^{-1} in the "Poor" site. Water electrical conductivity (0.24-0.35 mS cm^{-1}, i.e., 240-350 µS cm^{-1}) exceeded the guide's threshold of 215 µS cm^{-1} at all six sites, so it contributed no score and did not differentiate conditions. The water table was deeper in degraded sites (26.5 ± 4.9 cm; 21.1-36.2 cm) than in conserved sites (7.4 ± 3.3 cm; 2.2-13.6 cm; $F_{1,4}$ = 10.54; p = 0.031), with a mean difference of 19.1 cm (Table 2). These measurements agree with the scoring in Table 2: the three degraded sites received the lowest score for this indicator (10.3), and S5, with the shallowest water table (2.2 cm), received the highest (30.8). Peat was thinner in degraded sites (91.1 ± 1.7 cm; 88.4-94.2 cm) than in conserved sites (138.5 ± 9.0 cm; 125.4-155.8 cm; $F_{1,4}$ = 26.58; p =

215 0.007), a difference of 47.4 cm. Across sites, the water table was deeper where peat was thinner (r = -
216 0.86; p = 0.027; n = 6).

Table 2 Measured values, relative values of attributes and indicators, and bofedal ecosystem condition by sampling site

Attribute	Indicator	Degraded						Conserved					
		S1		S2		S3		S4		S5		S6	
		Meas.	Score	Meas.	Score	Meas.	Score	Meas.	Score	Meas.	Score	Meas.	Score
Water condition	Water table depth in dry season (cm)	36.2	10.3	21.1	10.3	22.2	10.3	13.6	20.5	2.2	30.8	6.3	20.5
	Electrical conductivity (mS cm^{-1})	0.28	0	0.35	0	0.25	0	0.25	0	0.28	0	0.24	0
Soil condition	Peat depth (cm)	88.4	3.1	94.2	3.1	90.7	3.1	125.4	6.1	134.2	6.1	155.8	6.1
	Organic matter (%)	21.33	3	21.1	3	21.07	3	23.27	3	23.87	3	22.97	3
	Bulk density (g cm^{-3})	0.37	1.2	0.23	2.3	0.17	3.5	0.24	2.3	0.16	3.5	0.21	2.3
	Signs of erosion (qualitative)	D	0	C	1	C	1	A	2.9	B	1.9	A	2.9
Biotic condition	Native species (%)	68	5.8	72	5.8	79	5.8	95	8.7	84	8.7	92	8.7
	Species richness (no. of species per area)	6	1	10	2.1	13	3.1	12	3.1	9	2.1	8	2.1
	Live vegetation cover (%)	45	0	50	0	55	0	95	2	90	2	95	2
	Aboveground biomass (kg DM ha^{-1})	960	3.4	992	3.4	1200	5.1	1586	5.1	1456	5.1	1536	5.1
Landscape alterations	Presence of degradation factors (qualitative)	C	2.7	C	2.7	C	2.7	A	8	B	5.3	A	8
	Hydrological connectivity of the bofedal (qualitative)	A	8	A	8	A	8	A	8	A	8	A	8
	Relative value (%)		**38.5**		**41.7**		**45.6**		**69.7**		**76.5**		**68.7**
	Bofedal condition		**Poor**		**Fair**		**Fair**		**Good**		**Good**		**Good**

Note. Meas.: value measured at the site; Score: relative value (weighted score) assigned according to the scale in the bofedal ecosystem condition assessment guide (MINAM 2019). Category ranges: Poor (20.1-40), Fair (40.1-60), and Good (60.1-80). For qualitative indicators, the measured value is the category assigned in the field.

Differences were concentrated in the indicators most sensitive to hydrological regime and grazing, whereas electrical conductivity, organic matter, and hydrological connectivity received the same relative value at all six sites (Table 2).

Spatiotemporal variation of carbon dioxide flux

FCO_2 was higher in degraded bofedales (1.10 ± 0.05 g CO_2 m^{-2} h^{-1}) than in conserved ones (0.89 ± 0.04 g CO_2 m^{-2} h^{-1}; $F_{1,4}$ = 11.56; p = 0.027), with a difference of 0.21 g CO_2 m^{-2} h^{-1} (95% CI: 0.04-0.38), equivalent to 23.6% (Table 3). Flux also varied among dates (p < 0.001), with no condition × date interaction (p = 0.084).

Table 3 Means of soil CO_2 flux, soil temperature and moisture, and micrometeorological variables in degraded (S1-S3) and conserved (S4-S6) bofedales

Variable	Degraded	Conserved	Condition	Date	C × D
FCO_2	1.10 ± 0.05[a]	0.89 ± 0.04[b]	0.027	< 0.001	0.084
ST (°C)	14.93 ± 0.47	14.58 ± 0.47	0.623	< 0.001	< 0.001
SM (%)	58.93 ± 2.51	65.88 ± 2.51	0.124	< 0.001	0.009
Tair (°C)	18.96 ± 0.47	17.34 ± 0.47	0.074	< 0.001	0.004
RH (%)	37.5 ± 0.8	40.4 ± 0.7	0.052	< 0.001	0.005
Ws (m s^{-1})	1.50 ± 0.23	1.90 ± 0.23	0.289	0.009	0.117
P (hPa)	601.5 ± 0.4	602.5 ± 0.4	0.125	< 0.001	0.733

Note. Values: mean ± standard error. Columns Condition, Date, and C × D show the p-value of the mixed model for condition, date, and their interaction (F tests with 1 and 4 degrees of freedom for condition and with 11 and 44 for date and interaction). Different letters indicate differences between conditions (p < 0.05). Sample size: n = 432 for FCO_2 and ST; n = 144 for SM and micrometeorological variables. FCO_2 (g CO_2 m^{-2} h^{-1}): soil CO_2 flux; ST: soil temperature; SM: soil moisture; Tair: air temperature; RH: relative humidity; Ws: wind speed; P: atmospheric pressure.

FCO_2 was higher (p < 0.05) on 25 October, 18 November, and 28 December 2025, and 6 and 26 February 2026 (1.15-1.18 g CO_2 m^{-2} h^{-1}) than on 10 and 30 August, 8 October, and 7 December 2025 (0.76-0.80 g CO_2 m^{-2} h^{-1}) (Fig. 2a). Mean FCO_2 of degraded bofedales exceeded that of conserved bofedales in all 12 campaigns, with the largest difference recorded on 26 February 2026 (0.62 g CO_2 m^{-2} h^{-1}) (Fig. 2a; Online Resource 1, Table S3). On some dates, however, the difference was minimal (0.04-0.07 g CO_2 m^{-2} h^{-1} on

30 August, 21 September, and 17 March; Online Resource 1, Table S3). Across sites and dates, means ranged from 0.58 to 1.76 g CO_2 m^{-2} h^{-1}.

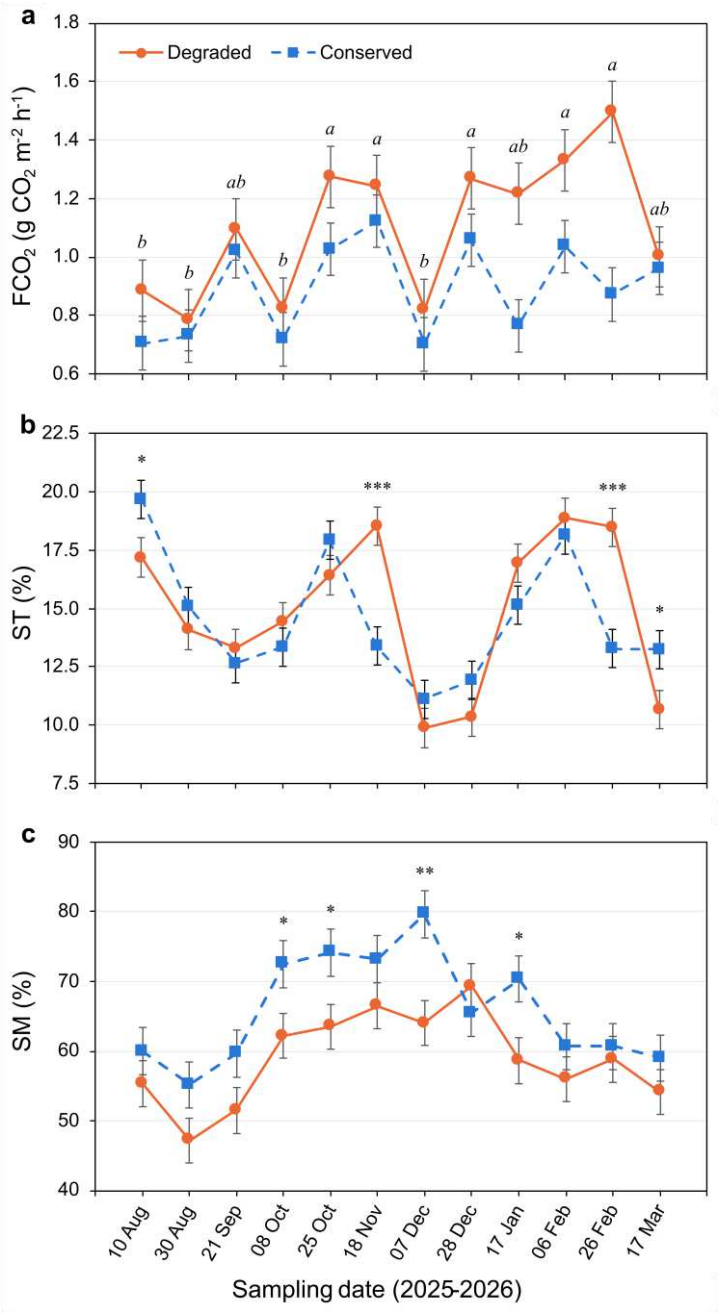

Fig. 2 Temporal variation of soil CO_2 flux (FCO_2; a), soil temperature (ST; b), and soil moisture (SM; c) in degraded and conserved high-Andean bofedales. Orange circles with solid line correspond to degraded bofedal, and blue squares with dashed line to conserved bofedal. Each symbol is the mean ± standard error of one condition on one date: 18 chambers in (a) and (b), and 6 recording positions in (c). In (a), dates sharing a letter do not differ from each other (Tukey, $\alpha = 0.05$). In (b) and (c), asterisks indicate dates on which both conditions differed (* $p < 0.05$; ** $p < 0.01$; *** $p < 0.001$)

The three degraded sites (S1-S3: 1.09-1.13 g CO_2 m^{-2} h^{-1}) had higher FCO_2 than the three conserved sites (S4-S6: 0.86-0.91 g CO_2 m^{-2} h^{-1}), and sites within the same condition had very similar values (Fig. 3). In degraded sites, the coefficient of variation of flux across chambers and dates combined was 35.4%, versus 31.1% in conserved sites (Online Resource 1, Table S2). This difference was driven mainly by S1 (CV = 41.1%).

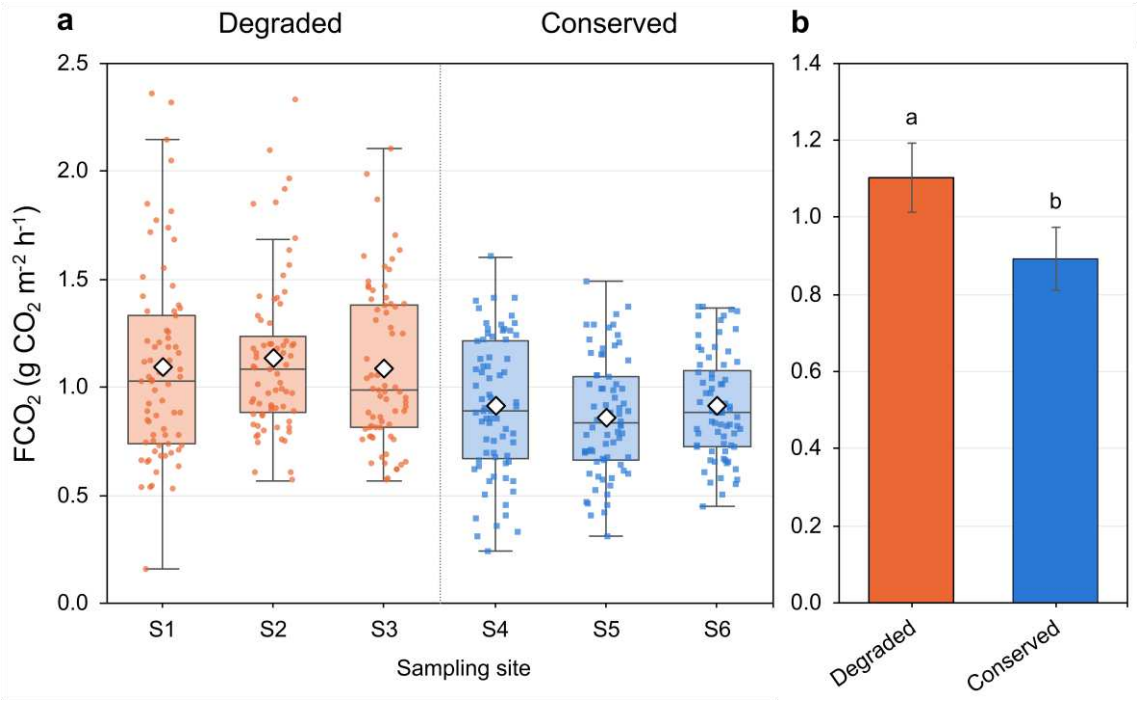

Fig. 3 Soil CO_2 flux (FCO_2) at the six sampling sites (a) and by conservation condition (b) of the bofedal. (a) Degraded sites (S1-S3, orange) and conserved sites (S4-S6, blue): boxes represent the median and interquartile range; whiskers, 1.5 times the interquartile range; points, individual measurements (n = 72 per site); diamonds, site mean. (b) Mean ± 95% confidence interval (n = 216 per condition); different letters indicate differences between conditions (p = 0.027)

Relationship of carbon dioxide flux with soil properties and micrometeorological variables in conserved and degraded bofedales

ST did not differ between degraded (14.9 °C) and conserved (14.6 °C; p = 0.623) bofedales, but the condition × date interaction was significant (p < 0.001). Degraded sites were 5.2 °C warmer on 18 November 2025 and 26 February 2026 (p < 0.001), and 2.5-2.6 °C colder on 10 August 2025 and 17 March 2026 (p < 0.05) (Fig. 2b). SM did not differ between conditions either (65.9% in conserved and 58.9% in degraded; p = 0.124), although the interaction was significant (p = 0.009), and conserved bofedales were wetter on 8 and 25 October, 7 December 2025, and 17 January 2026, with differences of

10.3-15.7 percentage points ($p < 0.05$) (Table 3; Fig. 2c). These differences were concentrated in the transition from the dry to the rainy season.

Tair (19.0 and 17.3 °C in degraded and conserved bofedales, respectively), Ws, and P did not differ between conditions ($p \geq 0.07$). RH tended to be higher in conserved (40.4%) than in degraded (37.5%; $p = 0.052$) sites, with a condition × date interaction ($p = 0.005$); it was higher in conserved sites on 30 August, 18 November, and 7 December 2025, and 26 February 2026, with differences of 7.6-11.6 percentage points ($p < 0.05$). All these variables varied among dates ($p \leq 0.009$) (Table 3; Online Resource 1, Table S4). OM, EC, pH, and BD did not differ between conditions ($p \geq 0.38$). pH was slightly alkaline in both conditions (7.67-7.80; Table 4).

Table 4 Soil properties (0-10 cm) by site and conservation condition at soil CO_2 flux measurement sites in high-Andean bofedales

Site	OM (%)	EC (mS cm^{-1})	pH	BD (g cm^{-3})
S1	21.33 ± 1.79	0.28 ± 0.03	7.94 ± 0.24	0.37 ± 0.30
S2	21.10 ± 8.42	0.35 ± 0.01	7.79 ± 0.04	0.23 ± 0.07
S3	21.07 ± 8.29	0.25 ± 0.02	7.30 ± 0.11	0.17 ± 0.09
Degraded	**21.17 ± 2.16**	**0.29 ± 0.02**	**7.67 ± 0.22**	**0.25 ± 0.05**
S4	23.27 ± 13.09	0.25 ± 0.01	7.60 ± 0.28	0.24 ± 0.21
S5	23.87 ± 2.83	0.28 ± 0.02	7.54 ± 0.03	0.16 ± 0.04
S6	22.97 ± 3.61	0.24 ± 0.01	8.27 ± 0.05	0.21 ± 0.02
Conserved	**23.37 ± 2.16**	**0.26 ± 0.02**	**7.80 ± 0.22**	**0.20 ± 0.05**

Note. Sites: mean ± standard deviation (n = 3). Condition: mean ± standard error of a linear mixed model (n = 18 samples). No difference was significant ($p > 0.05$). OM: organic matter; EC: electrical conductivity; BD: bulk density. The high standard deviation of BD in S1 (0.37 ± 0.30) and S4 (0.24 ± 0.21), and of OM in S2, S3, and S4 (± 8.3 to 13.1%), reflects peat heterogeneity within each site (n = 3) and limits comparison.

Within each recording unit, FCO_2 correlated positively with ST ($r_{rm} = 0.21$; $p < 0.001$) and with RH ($r_{rm} = 0.19$; $p = 0.032$). RH was the only variable that retained an association when entered as a covariate in the mixed model: per standard deviation, FCO_2 increased by 0.098 g CO_2 m^{-2} h^{-1} ($p = 0.005$). ST, in contrast, lost its association ($p = 0.373$). SM, Tair, Ws, and P did not correlate with flux ($p \geq 0.097$). Among soil properties, only OM showed a relationship, and it was negative. Within each site, samples with more OM were associated with lower FCO_2 ($r_{rm} = -0.63$; $p = 0.021$; 18 samples from 6 sites). The same trend was

observed across sites, although differences were not significant: conserved sites had slightly more OM and lower fluxes. EC, BD, and pH were not related to FCO_2 ($p \geq 0.11$; Table 5; Fig. 4).

Table 5 Repeated-measures correlation between edaphic and micrometeorological variables and soil CO_2 flux in conserved and degraded high-Andean bofedales of Jila Cajamarca, Puno

Variable	Coef.	Value	p
ST	r_{rm}	0.21	< 0.001
SM	r_{rm}	0.14	0.097
Tair	r_{rm}	0.00	0.992
RH	r_{rm}	0.19	0.032
Ws	r_{rm}	0.06	0.459
P	r_{rm}	0.06	0.516
OM	r_{rm}	-0.63	0.021
EC	r_{rm}	0.24	0.42
pH	r_{rm}	0.21	0.49
BD	r_{rm}	0.46	0.11

Note. r_{rm}: repeated-measures correlation (Bakdash and Marusich 2017). It measures association within each recording unit, which for ST were 36 chambers and for micrometeorological variables and SM, 12 recording positions. For OM, EC, pH, and BD, the unit was the site (18 samples from 6 sites). FCO_2: soil CO_2 flux; ST: soil temperature; SM: soil moisture; Tair: air temperature; RH: relative humidity; Ws: wind speed; P: atmospheric pressure; OM: organic matter; EC: electrical conductivity; BD: bulk density.

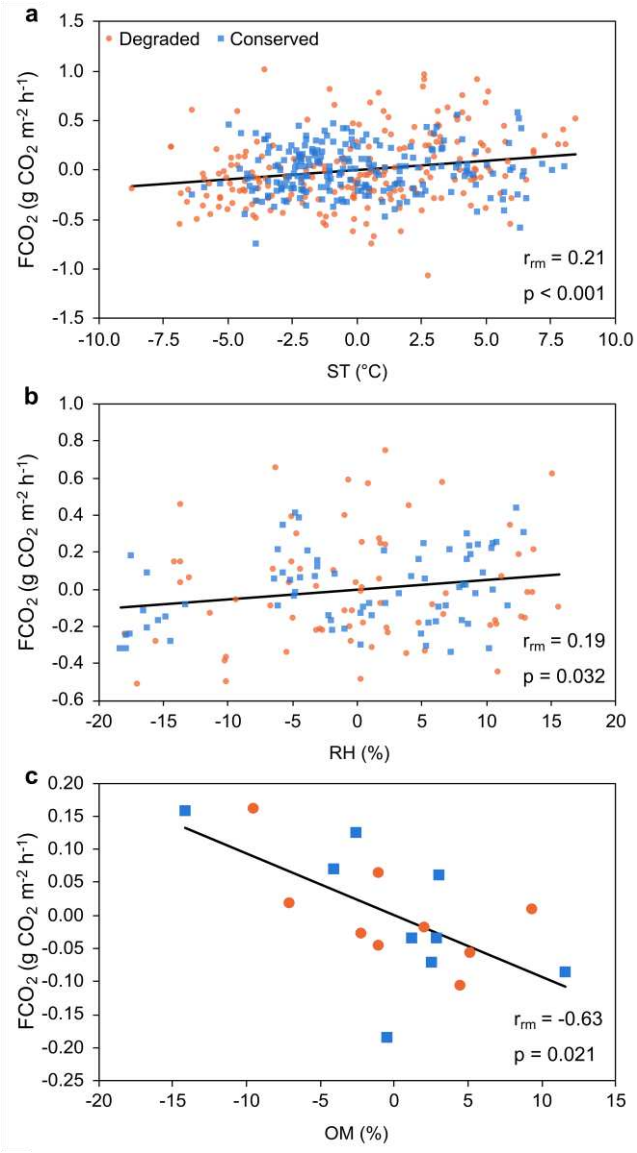

Fig. 4 Relationship of soil CO_2 flux (FCO_2) with soil temperature (ST; a), relative humidity (RH; b), and organic matter (OM; c) in degraded and conserved high-Andean bofedales. Degraded: orange circles; conserved: blue squares. In (a) and (b), values were centered on the mean of each chamber (a; n = 432) or each recording position (b; n = 144), and the line represents the common slope (a: $r_{rm} = 0.21$, $p < 0.001$; b: $r_{rm} = 0.19$, $p = 0.032$). In (c), each symbol is a soil sample (n = 18), with OM and FCO2 centered on the mean of their site ($r_{rm} = -0.63$; $p = 0.021$)

Discussion

Hydrological and vegetation indicators of bofedal degradation

The uniform relative values of electrical conductivity, organic matter, and hydrological connectivity across the six sites (Table 2) help to clarify how degradation operates in this bofedal. All sites exceeded

312 the guide's EC threshold, which, together with the slightly alkaline soil pH (Table 4), suggests inputs of
313 dissolved salts from the substrate or groundwater rather than an effect of degradation. Degradation
314 therefore appears to act on surface hydrology and vegetation without interrupting the wetland's
315 hydrological connection. Loss of vegetation cover in bofedales has also been documented in the Río
316 Zapatilla micro-watershed (Huanca 2024), and in the Río Pichacani watershed most bofedales showed a
317 favorable condition associated with vegetation cover, aboveground biomass, and hydrological
318 connectivity (Nina 2026).

319 The lower scores for water table and vegetation cover at degraded sites coincide with degradation
320 mechanisms documented in grazed and drained Andean peatlands (Sánchez et al. 2017; Planas-Clarke et
321 al. 2020), and with the strong dependence of water table level in these wetlands on precipitation and
322 groundwater inputs (Cooper et al. 2019). In the studied bofedal, the water table was at 21-36 cm depth in
323 degraded sites and at 2-14 cm in conserved sites, consistent with lower surface saturation in degraded
324 sectors. The absence of scorable live vegetation cover and the shallower peat (91.1 vs. 138.5 cm) in
325 degraded sites indicate loss of the peat-forming cushion-plant layer, the primary symptom of Puna
326 bofedal degradation due to overgrazing, drainage, and peat extraction (Maldonado 2014; Salvador et al.
327 2014).

328 The negative relationship between water table depth and peat thickness ($r = -0.86$) suggests that water
329 table decline and peat loss advance together, although with six sites it is not possible to separate cause
330 from effect. Floristic composition reinforces this interpretation: peat-forming cushion plants (*Distichia*
331 *muscoides* and *Oxychloe andina*) appeared among the dominant species only in “Good” condition sites,
332 whereas degraded sites were dominated by *Plantago tubulosa*, *Phylloscirpus deserticola*, and mosses, a
333 replacement that has been described in Puna bofedales subjected to intensive grazing and surface
334 desiccation (Maldonado 2014; Salvador et al. 2014). In a high-Andean peatland in Colombia, small-scale
335 experimental disturbances increased decomposition rates and facilitated the entry of invasive species
336 (Urbina and Benavides 2015), suggesting that replacement of cushion plants may in turn accelerate
337 carbon loss. The dominance of *Festuca dolichophylla* in conserved sites suggests a mixed-type bofedal,
338 with tussock grasses on wet peat.

Higher carbon dioxide flux in degraded sectors

The mean flux of conserved sectors, 0.89 g CO_2 m^{-2} h^{-1}, falls within the range recorded with the same equipment in the wetland of the Inner Bay of Puno, 0.67-0.99 g CO_2 m^{-2} h^{-1} (Flores-Aroni et al. 2025), whereas that of degraded sectors exceeds it. Both values are higher than those of tundra and Nothofagus forest soils in Patagonia, 0.35-0.81 g CO_2 m^{-2} h^{-1} (Sá et al. 2019), and approach those of non-degraded alpine wet meadows of Tibet during the growing season, 1.12-1.25 g CO_2 m^{-2} h^{-1} (Li et al. 2019). Because measurements were made between 09:00 and 14:00 h, when the soil is warmest, these values represent daytime rates and should not be extrapolated to daily or annual totals without considering the diel cycle of flux (Pavelka et al. 2018).

The higher FCO_2 of degraded sectors could be explained by the loss of water saturation, which favors aerobic peat decomposition. In degraded sites, the dry-season water table was, on average, 19.1 cm deeper (26.5 vs. 7.4 cm; Table 2) and SM was up to 15.7 percentage points lower in four campaigns (Fig. 2c), conditions that facilitate oxygen diffusion into carbon-rich horizons and stimulate microbial mineralization. In Cordillera Blanca peatlands, heavily drained sectors shifted from sinks to CO_2 sources (Planas-Clarke et al. 2020), and the global synthesis by Evans et al. (2021) identified water table depth as the dominant control on emissions from disturbed peatlands. At the global scale, water table decline increases CO_2 emissions and reduces CH_4 emissions, with a warming balance dominated by CO_2 (Huang et al. 2021). In the Amazon estuary, FCO_2 was higher on high topography, with the water table at about 31 cm depth (comparable to that of the degraded sites in this study, 21.1-36.2 cm), than in the flooded low topography (Flores et al. 2026); similarly, upland soils emitted more CO_2 than várzea (seasonally flooded floodplain) soils under açaí cultivation during the rainy season (Flores et al. 2025). In Peruvian Amazonian peatlands, degradation also increased CO_2 emissions (Lent et al. 2019). These studies consistently indicate that reduced water saturation is the most plausible mechanism behind the higher flux observed in degraded sites of the studied bofedal.

This result contrasts with that of Li et al. (2019), who found that degradation of alpine wet meadows reduced soil respiration by decreasing plant biomass and organic carbon. In the studied bofedal, degraded sites received no score for live vegetation cover (45-55%; Table 2), had lower aboveground biomass (960-1,200 vs. 1,456-1,586 kg DM ha^{-1}), and lacked litter (Online Resource 1, Table S5), yet they emitted more CO_2. This suggests that heterotrophic respiration of exposed peat, rather than root respiration, sustains the flux in these sectors, a hypothesis that should be confirmed by separating autotrophic and

heterotrophic respiration sources in future studies, for example through root exclusion or isotopic techniques (Kuzyakov 2006).

Seasonal modulation and variability of flux

The higher flux of degraded sectors persisted across all 12 campaigns over the eight months of monitoring, consistent with the nonsignificant condition × date interaction; this systematic difference points to a persistent effect of degradation on flux, even on the dates when the gap between conditions was minimal. Several of the campaigns with lower flux coincided with low temperatures or higher soil moisture. The clearest case was 7 December 2025, with the lowest soil temperature of the period and, in conserved sectors, the highest moisture (Fig. 2b, c). This pattern aligns with the lower microbial activity observed under low temperatures and frost in Puno bofedales (Nuñez 2024). It also coincides with the finding that, in wetlands of the region, the highest fluxes are recorded during the rainy season (Checalla 2023; Flores-Aroni et al. 2025), provided the soil does not become saturated. This suggests that, in the Altiplano, thermal and hydrological seasonality modulates flux with greater amplitude than conservation condition, without nullifying the main effect of degradation.

The greater flux variability in degraded sectors suggests a stronger response to temperature and moisture fluctuations, which near-permanent saturation (water table at 2-14 cm below the surface) buffers in conserved sites. This buffering effect is consistent with the dependence of the thermal sensitivity of respiration on position along the hydrological gradient (Yu et al. 2020).

Edaphic and micrometeorological controls on flux

Although mean ST was similar, degraded sectors warmed more on warm days and cooled more on cold days, possibly because a surface with less water, lower vegetation cover, and no litter has lower heat capacity and insulation. Similarly, the higher SM of conserved sectors during the transition to the rainy season reflects the greater water retention of little-altered peat. OM tended to be higher and BD lower in conserved sectors; these trends are consistent with the role of water saturation in carbon accumulation: in central Andean bofedales, soil organic carbon correlated negatively with dissolved oxygen, pH, and soil water temperature (Monge-Salazar et al. 2022), and carbon accumulation in high-Andean bofedales responds to changes in the hydroclimatic regime (Huaman et al. 2020). The trend toward higher BD in degraded sites is compatible with compaction by livestock trampling described in grazed peatlands

(Sánchez et al. 2017), and the stability of pH coincides with observations in Puno wetlands, where this variable changed little between seasons (Flores-Aroni et al. 2025).

Micrometeorological variables mainly reflected the seasonal transition between the dry and rainy seasons, rather than differences between conditions. The slightly higher RH over conserved sectors is consistent with evaporation from a saturated, vegetated surface, and its variation among dates agrees with the seasonal changes described in bofedales and wetlands of Puno (Nuñez 2024).

Within each chamber, FCO_2 increased with ST, but the relationship was weak and disappeared when ST was included as a covariate in the mixed model. Rather than a direct thermal control, both variables appear to have changed together over the season. Other studies did find a closer link. In Patagonian tundra soils, with mean temperatures of 4-8 °C, temperature explained more than 70% of flux variation (Sá et al. 2019). In the Inner Bay of Puno, flux correlated with soil temperature ($r = 0.49$) and air temperature ($r = 0.51$) (Flores-Aroni et al. 2025). Here, Tair showed no relationship at all. Two factors could explain this: measurements were made within a narrow time window, and saturated soil buffers changes in air temperature. With a mean ST near 15 °C during measurements, temperature appears less limiting than oxygen availability, consistent with the attenuation of the thermal sensitivity of decomposition by oxygen scarcity in saturated soils (Davidson and Janssens 2006). The lack of a linear relationship with SM does not rule out a water effect: in Amazonian peatlands respiration peaked at intermediate moisture levels (Lent et al. 2019), and in flooded soils of the Amazon estuary excess water reduced flux (Flores et al. 2026). In mineral soils, aerobic CO_2 production is maximal at about 60% water-filled pore space (WFPS) and declines toward saturation (Linn and Doran 1984). These findings suggest a nonlinear relationship between moisture and respiration, which the present study did not formally evaluate; expressing moisture as WFPS, from the SM and BD already measured, would allow it to be evaluated with the available data. The positive association with RH, the only micrometeorological variable related to flux, suggests that, in the Altiplano, atmospheric humidity accompanies the rainy-season conditions that favor soil biological activity. In Puno bofedales, flux has also been related to RH (Flores 2023) and to the combined effect of air temperature, RH, and light intensity (Checalla 2023). In contrast, in the Amazon estuary, where excess water limits respiration, FCO_2 was negatively associated with RH (Flores et al. 2026). The contrast suggests that the sign of the relationship depends on whether water limits or favors biological activity in each ecosystem.

The negative correlation between FCO_2 and OM, the substrate for heterotrophic respiration, appears contradictory; however, OM tends to be higher where the soil is more saturated and less compacted, that is, where flux is lower. Therefore, rather than directly controlling flux, OM may reflect the greater saturation that limits decomposition (Monge-Salazar et al. 2022). In Puno bofedales, soils with higher OM and organic carbon are in better ecological condition and retain more carbon (Flores 2023; Mamani 2024).

Conclusions

Conserved sites of the bofedal were classified as "Good," and degraded sites as "Fair" and, in one case (S1), "Poor." These differences were concentrated in the indicators most sensitive to hydrological regime and grazing, particularly dry-season water table depth, peat depth, and live vegetation cover, and were reflected in the vegetation: cushion plants (*Distichia muscoides* and *Oxychloe andina*) and litter were recorded only at conserved sites, whereas *Plantago tubulosa* dominated at degraded sites. The water table was, on average, at 26.5 cm depth in degraded sites and at 7.4 cm in conserved sites, and peat was 47.4 cm thinner in the former (91.1 vs. 138.5 cm).

Soil CO_2 flux was 23.6% higher in degraded sectors (1.10 g CO_2 m^{-2} h^{-1}) than in conserved sectors (0.89 g CO_2 m^{-2} h^{-1}). The difference persisted across all 12 campaigns, with no condition × date interaction. Soil properties did not differ between conditions; among micrometeorological variables, only relative humidity tended to be higher in conserved sectors, and soil temperature and moisture differed only in some campaigns. Relative humidity, positively, and organic matter, negatively, were the variables most consistently associated with CO_2 flux, and the association with organic matter held within each site. The association with soil temperature was weak and did not hold when soil temperature was included as a covariate in the mixed model. However, the negative relationship with organic matter should be interpreted with caution, given the small sample size (18 samples from 6 sites) and its possible confounding with the water saturation gradient.

Bofedal degradation was associated with higher daytime soil CO_2 emissions, suggesting that conservation and hydrological restoration of high-Andean bofedales could reduce soil CO_2 emissions. These results should be interpreted bearing in mind that measurements were restricted to daytime hours (09:00-14:00 h) and to an eight-month period, and therefore do not allow estimation of annual carbon balances. Future studies should incorporate methane, continuous water table monitoring, and the diel cycle of flux to

455 establish the net GHG balance of these ecosystems. It would also be advisable to separate autotrophic and
456 heterotrophic respiration sources and to increase the number of sites per condition to improve statistical
457 power.

458 **References**

459 Anderson TG, Christie DA, Chávez RO et al (2021) Spatiotemporal peatland productivity and climate
460 relationships across the western South American Altiplano. J Geophys Res Biogeosciences
461 126:e2020JG005994. https://doi.org/10.1029/2020JG005994

462 Bakdash JZ, Marusich LR (2017) Repeated measures correlation. Front Psychol 8:.
463 https://doi.org/10.3389/fpsyg.2017.00456

464 Beck HE, Zimmermann NE, McVicar TR et al (2018) Present and future Köppen-Geiger climate
465 classification maps at 1-km resolution. Sci Data 5:180214.
466 https://doi.org/10.1038/sdata.2018.214

467 Checalla J (2023) Flujo de dióxido de carbono del suelo en el bofedal del sector Pampa Uta, en el distrito
468 de Capaso - El Collao, 2022. Undergraduate thesis, Universidad Privada San Carlos

469 Cooper DJ, Sueltenfuss J, Oyague E et al (2019) Drivers of peatland water table dynamics in the central
470 Andes, Bolivia and Peru. Hydrol Process 33:1913–1925. https://doi.org/10.1002/hyp.13446

471 Davidson EA, Janssens IA (2006) Temperature sensitivity of soil carbon decomposition and feedbacks to
472 climate change. Nature 440:165–173. https://doi.org/10.1038/nature04514

473 Davidson EA, Verchot LV, Cattanio JH et al (2000) Effects of soil water content on soil respiration in
474 forests and cattle pastures of eastern Amazonia. Biogeochemistry 48:53–69.
475 https://doi.org/10.1023/A:1006204113917

476 Embrapa (2017) Manual de métodos de análises de solo, 3rd edn. Teixeira, P. C. Donagemma, G. K.
477 Fontana, Ademir Teixeira, W. G., Brasília, DF

478 Evans CD, Peacock M, Baird AJ et al (2021) Overriding water table control on managed peatland
479 greenhouse gas emissions. Nature 593:548–552. https://doi.org/10.1038/s41586-021-03523-1

Flores M (2023) Dinámica del flujo de dióxido de carbono del suelo en el bofedal de la Moya, en el distrito de Ayaviri - Melgar, 2022. Undergraduate thesis, Universidad Privada San Carlos

Flores M, Cattanio JH, Carvalho CJR (2025) Dynamics of greenhouse gas fluxes in açaí cultivation: Comparing Amazonian upland and floodplain soils. Forests 16:944. https://doi.org/10.3390/f16060944

Flores M, Cattanio JH, Jardim MAG et al (2026) Greenhouse gas fluxes in a managed floodplain forest in the Amazon estuary. Agric For Meteorol 378:110979. https://doi.org/10.1016/j.agrformet.2025.110979

Flores-Aroni M, Ccama C, Cattanio JH (2025) Dinámica del flujo de dióxido de carbono del suelo en el humedal de la Bahía Interior de Puno. Rev Investig Altoandinas - J High Andean Res 27:e27679. https://doi.org/10.18271/ria.2025.679

Hribljan JA, Hough M, Lilleskov EA et al (2024) Elevation and temperature are strong predictors of long-term carbon accumulation across tropical Andean mountain peatlands. Mitig Adapt Strateg Glob Change 29:1. https://doi.org/10.1007/s11027-023-10089-y

Huaman Y, Moreira-Turcq P, Espinoza R et al (2020) Influencia de los cambios climáticos en la acumulación de carbono en Bofedales Altoandinos durante los últimos 2 500 años. Ecol Apl 19:35–41. https://doi.org/10.21704/rea.v19i1.1444

Huanca EY (2024) Determinación de la cobertura vegetal de los bofedales en la microcuenca del rio Zapatilla, El Collao, Puno. Undergraduate thesis, Universidad Nacional del Altiplano

Huang Y, Ciais P, Luo Y et al (2021) Tradeoff of CO2 and CH4 emissions from global peatlands under water-table drawdown. Nat Clim Change 11:618–622. https://doi.org/10.1038/s41558-021-01059-w

Hurlbert SH (1984) Pseudoreplication and the design of ecological field experiments. Ecol Monogr 54:187–211. https://doi.org/10.2307/1942661

IPCC (2021) Climate Change 2021: The Physical Science Basis. Contribution of Working Group I to the Sixth Assessment Report of the Intergovernmental Panel on Climate Change. Cambridge University Press, Cambridge (UK)

IPCC (2014) Climate Change 2014: Synthesis Report. Contribution of Working Groups I, II and III to the Fifth Assessment Report of the Intergovernmental Panel on Climate Change. Geneva

Kalra YP, Maynard DG (1991) Methods manual for forest soil and plant analysis. Information Report NOR-X-319E, Forestry Canada, Northwest Region, Northern Forestry Centre

Kuzyakov Y (2006) Sources of CO2 efflux from soil and review of partitioning methods. Soil Biol Biochem 38:425–448. https://doi.org/10.1016/j.soilbio.2005.08.020

Leifeld J, Menichetti L (2018) The underappreciated potential of peatlands in global climate change mitigation strategies. Nat Commun 9:1071. https://doi.org/10.1038/s41467-018-03406-6

Lent J, Hergoualc'h K, Verchot L et al (2019) Greenhouse gas emissions along a peat swamp forest degradation gradient in the Peruvian Amazon: soil moisture and palm roots effects. Mitig Adapt Strateg Glob Change 24:625–643. https://doi.org/10.1007/s11027-018-9796-x

Li Z, Gao J, Wen L et al (2019) Dynamics of soil respiration in alpine wetland meadows exposed to different levels of degradation in the Qinghai-Tibet Plateau, China. Sci Rep 9:7469. https://doi.org/10.1038/s41598-019-43904-1

Linn DM, Doran JW (1984) Effect of water-filled pore space on carbon dioxide and nitrous oxide production in tilled and nontilled soils. Soil Sci Soc Am J 48:1267–1272. https://doi.org/10.2136/sssaj1984.03615995004800060013x

Maldonado M (2014) An introduction to the bofedales of the Peruvian High Andes. Mires Peat 15:1–13

Mamani M (2024) Reserva de carbono y emisión de dióxido de carbono del bofedal en el sector Vizcachani, distrito de Capaso, El Collao - 2022. Undergraduate thesis, Universidad Privada San Carlos

Marthews TR, Riutta T, Oliveras I et al (2014) Measuring tropical forest carbon allocation and cycling: A RAINFOR-GEM field manual for intensive census plots (v3.0), Global Ecosystems Monitoring network. Global Ecosystems Monitoring network

Metcalfe DB, Meir P, Aragão LEOC et al (2007) Factors controlling spatio-temporal variation in carbon dioxide efflux from surface litter, roots, and soil organic matter at four rain forest sites in the eastern Amazon. J Geophys Res Biogeosciences 112:. https://doi.org/10.1029/2007JG000443

MINAM (2019) Guía de evaluación del estado del ecosistema de bofedal. Ministerio del Ambiente, Lima

Monge-Salazar MJ, Tovar C, Cuadros-Adriazola J et al (2022) Ecohydrology and ecosystem services of a natural and an artificial bofedal wetland in the central Andes. Sci Total Environ 838:155968. https://doi.org/10.1016/j.scitotenv.2022.155968

Nina FE (2026) Análisis multitemporal de la cobertura vegetal de los bofedales altoandinos en la cuenca del río Pichacani - Puno, período 2008 - 2023. Undergraduate thesis, Universidad Privada San Carlos

Nuñez C (2024) Variabilidad espacial y temporal del flujo de dióxido de carbono del bofedal del sector Ccalluchani, Pichacani, Puno - 2024. Undergraduate thesis, Universidad Privada San Carlos

Oyague E, Cooper D (2020) Peatlands of the Central Andes Puna, South America. Wetl Sci Pract 37:255–260. https://doi.org/10.1672/UCRT083-204

Pavelka M, Acosta M, Kiese R et al (2018) Standardisation of chamber technique for CO2, N2O and CH4 fluxes measurements from terrestrial ecosystems. Int Agrophysics 32:569–587. https://doi.org/10.1515/intag-2017-0045

Planas-Clarke AM, Chimner RA, Hribljan JA et al (2020) The effect of water table levels and short-term ditch restoration on mountain peatland carbon cycling in the Cordillera Blanca, Peru. Wetl Ecol Manag 28:51–69. https://doi.org/10.1007/s11273-019-09694-z

Pribyl DW (2010) A critical review of the conventional SOC to SOM conversion factor. Geoderma 156:75–83. https://doi.org/10.1016/j.geoderma.2010.02.003

R Core Team (2025) R: A language and environment for statistical computing (Version 4.5.1). R Foundation for Statistical Computing, Vienna. https://www.r-project.org/

Raich JW, Schlesinger WH (1992) The global carbon dioxide flux in soil respiration and its relationship to vegetation and climate. Tellus B 44:81–99. https://doi.org/10.1034/j.1600-0889.1992.t01-1-00001.x

Ramsar (2018) Perspectiva mundial sobre los humedales: Estado de los humedales del mundo y de los servicios que prestan a las personas. Secretaría de la Convención de Ramsar, Gland (Suiza)

Sá MMF, Schaefer CEGR, Loureiro DC et al (2019) Fluxes of CO2, CH4, and N2O in tundra-covered and Nothofagus forest soils in the Argentinian Patagonia. Sci Total Environ 659:401–409. https://doi.org/10.1016/j.scitotenv.2018.12.328

Salvador F, Monerris J, Rochefort L (2014) Peatlands of the Peruvian Puna ecoregion: types, characteristics and disturbance. Mires Peat 15:1–17. https://doi.org/10.19189/001c.128517

Sánchez ME, Chimner R, Hribljan J et al (2017) Carbon dioxide and methane fluxes in grazed and undisturbed mountain peatlands in the Ecuadorian Andes. Mires Peat 19:1–18. https://doi.org/10.19189/MaP.2017.OMB.277

SENAMHI (2026) Datos meteorológicos. https://www.gob.pe/senamhi

Urbina JC, Benavides JC (2015) Simulated small scale disturbances increase decomposition rates and facilitates invasive species encroachment in a high elevation Tropical Andean Peatland. Biotropica 47:143–151. https://doi.org/10.1111/btp.12191

Walkley A, Black IA (1934) An examination of the Degtjareff method for determining soil organic matter, and a proposed modification of the chromic acid titration method. Soil Sci 37:29–38. https://doi.org/10.1097/00010694-193401000-00003

Yu L, Wang H, Wang Y et al (2020) Temporal variation in soil respiration and its sensitivity to temperature along a hydrological gradient in an alpine wetland of the Tibetan Plateau. Agric For Meteorol 282–283:107854. https://doi.org/10.1016/j.agrformet.2019.107854

Statements and Declarations

Funding

This research received no external funding.

Competing interests

The authors declare that they have no conflicts of interest.

Author contributions

Mario Flores-Aroni: Conceptualization, Methodology, Formal analysis, Data curation, Visualization, Writing - original draft, Writing - review & editing. Alcida Lourdes Chua Mamani: Investigation (fieldwork), Data curation, Formal analysis. José Henrique Cattanio: Supervision, Validation, Writing - review & editing. All authors read and approved the final manuscript.

Data availability

The datasets generated and/or analysed during the current study are available from the corresponding author on reasonable request.

Acknowledgments

We thank the Biogeochemical Cycles Laboratory of the Graduate Program in Environmental Sciences of the Federal University of Pará (Belém, Brazil) for providing the carbon dioxide flux measurement equipment. We thank Dr. Edson Efraín Tito Quispe for his support in fieldwork and in the identification of plant species.

Supplementary Files

This is a list of supplementary files associated with this preprint. Click to download.

- OnlineResourceSpatiotemporalsoilCO2fluxbofedal.docx